Analytica Chimica Acta xxx (2018) 1–10

Contents lists available at ScienceDirect

Analytica Chimica Acta

journal homepage: www.elsevier.com/locate/aca

Electrochemical quantitation of *Leishmania infantum* based on detection of its kDNA genome and transduction of non-spherical gold nanoparticles

R. Nazari-Vanani [a], N. Sattarahmady [a, b], H. Yadegari [c], N. Delshadi [a, d], G.R. Hatam [e], H. Heli [a, *]

[a] Nanomedicine and Nanobiology Research Center, Shiraz University of Medical Sciences, Shiraz, Iran
[b] Department of Medical Physics, School of Medicine, Shiraz University of Medical Sciences, Shiraz, Iran
[c] Department of Mechanical and Materials Engineering, University of Western Ontario, London, Ontario N6A 5B9, Canada
[d] Fars Academic Center for Education, Culture and Research, Shiraz, Iran
[e] Department of Parasitology and Mycology, School of Medicine, Shiraz University of Medical Sciences, Shiraz, Iran

HIGHLIGHTS

- Non-spherical gold nanoparticles were electrodeposited.
- The nanoparticles were employed to fabricate a *Leishmania infantum* DNA sensor.
- The DNA sensor was applied to detect clinical samples.

GRAPHICAL ABSTRACT

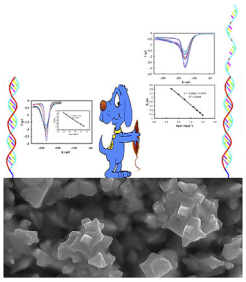

ARTICLE INFO

Article history:
Received 1 December 2017
Received in revised form
28 June 2018
Accepted 21 August 2018
Available online xxx

Keywords:
L. infantum
Leishmaniasis
DNA biosensor
Gold nanostructure
Toluidine blue
Electrochemical sensor
Nucleic acid

ABSTRACT

Detecting and monitoring the pathogens with high selectivity and sensitivity is critical for public health. In the present study, we demonstrated a specific analytical strategy for sensitive detection of *Leishmania infantum* genome. The developed sensor utilized toluidine blue as a hybridization indicator and a *Leishmania infantum*-specific capture DNA sequence immobilized on a high-surface area gold nanostructure as an electrochemical transducer. The produced analytical response was based on the hybridization of the single-stranded DNA from the target with the immobilized DNA sequence at the electrode surface. The developed DNA sensor in this study was successfully employed to detect a synthetic *Leishmania infantum* target sequence in a wide concentration range from 1×10^{-18} to 1×10^{-10} mol L^{-1} with a detection limit of 0.2 amol L^{-1} with the ability to discriminate the target sequence from mismatched sequences. Moreover, the designed DNA sensor showed a good reproducibility and stability during repeated regeneration and hybridization cycles. The DNA sensor could detect *Leishmania infantum* genome in a wide concentration range from 15 to 50 ng μL^{-1} with a detection limit of 29 ng μL^{-1}. Furthermore, clinical trials confirmed the applicability of the developed DNA sensor for practical applications.

* Corresponding author.
E-mail addresses: heli@sums.ac.ir, hheli7@yahoo.com (H. Heli).

https://doi.org/10.1016/j.aca.2018.08.036
0003-2670/

1. Introduction

Quality of life is closely dependent on the ability of mankind for diseases control. Therefore, developing fast, sensitive and continues monitoring techniques for detecting pathogens are of great importance in public health [1]. Conventional detection methods for microorganisms and toxins in food, water, and human specimens generally require hours or days of operation by trained personnel and usually result in inconclusive identification [2]. Accordingly, considerable deal of efforts has been directed towards the development of new techniques capable of rapid detection of pathogens at low concentrations [3–10].

Leishmaniasis is a group of diseases caused by obligate intracellular protozoa of the genus *Leishmania*. *Leishmania* appears in three different forms of visceral (VL), cutaneous (CL), and mucocutaneous leishmaniasis [11]. VL form, also known as black sickness or kala-azar, is the most severe form of the disease with estimated 500000/year new cases in less developed countries [12–14]. VL is typically caused by *Leishmania donovani* complex, which comprises three species: *Leishmania donovani*, *Leishmania infantum* (*L. infantum*), and *Leishmania chagasi*. *L. infantum* is responsible for VL in multiple areas of the world where dogs are considered as the major reservoir host for human *Leishmania* infections [15]. Human VL has recently emerged as an opportunistic infection among individuals co-infected with human immunodeficiency virus (HIV)/AIDS as well as in persons taking immunosuppressive drugs [15,16]. VL is characterized by prolonged fever, splenomegaly, hepatomegaly, substantial weight loss, progressive anemia, hypergammaglobulinemia, pancytopenia, accompanied by serious infections. Therefore, accurate diagnosis is critical for VL control as well as identification of treatment failure [17].

Various laboratory diagnosis routes have been established for leishmaniasis including (i) detection of parasite in tissues by conducting optical microscopic examination on the stained specimen, in vitro culture, or animal inoculation; (ii) detection of parasite DNA in tissue samples; (iii) immunodiagnosis through detection of parasite antigen in clinical samples by tracing nonspecific or specific anti-*Leishmania* antibodies (immunoglobulin), or by assay for *Leishmania*-specific cell-mediated immunity [11,18]. These tests can be exclusively performed in well-equipped laboratories or hospitals, demanding high-end instrumentations, trained personnel, complicated sample pretreatment and long analysis periods [19]. Therefore, developing simpler and less-invasive alternatives for diagnosis of leishmaniasis may facilitate the detection of the disease and reduce the analysis time.

Several detection methods have been reports for *Leishmania* parasites. A real-time PCR (rtPCR) technique found positive results in 47% of clinically leishmaniotic dogs, whereas all samples from healthy dogs were found to be negative [20]. The rtPCR assay was also applied for detection of *L. infantum* in canine blood samples with an analytical sensitivity of 0.1 fg of DNA equivalent to 0.002 parasite per reaction [14]. Moreover, rtPCR has been shown to detect *L. infantum* in 96.7% of dogs without clinical signs and 100% of symptomatic ones [21]. Besides, multiple DNA biosensors have been also fabricated in our research group for identification of *Leishmania major* using different electrochemical detection based on gold nanoparticles with photometric detection [4], ferrite quantum dots [5], gold nanoleaves [6] or gold hierarchical nanoleaflets [9]. Furthermore, a SPR immunosensor was developed using an 11-mercaptoundecanoic acid modified gold chip for detection of anti-*L. infantum* antibodies [22]. An immunofluorescent antibody test (IFAT), enzyme-linked immunosorbent assay (ELISA) and Western blot have been explored for diagnosis of clinical feline leishmaniosis [23]. IFAT displayed higher sensitivity compared to ELISA (75 vs 70%) for the detection of subclinical infection, while ELISA was better for diagnosing clinical leishmaniosis (98 vs 97%).

Meanwhile, nanomaterials exhibit unique characteristics arising from their shape, size, aspect ratio and surface functionalization properties [24–26]. Thus, considerable amount of research attentions have been devoted towards application of nanomaterials to fabricate different types of biosensors as more efficient alternatives for conventional diagnosis techniques. The resultant biosensors provide improved characteristics in terms of specificity, sensitivity, size and cost [3–10,24–26]. On the other hand, the successful design and development of biosensors requires involvement and combination of different disciplines to achieve the desired performance [27]. As for the biosensors, those based on hybridization of complementary DNA sequences (the genosensors) have been vastly investigated by different transduction routs of photonic [4,8], electrochemical [7] and mass changes [27]. In this regard, tremendous efforts have been performed by researches to employ high-surface area-substrates for the immobilization of detecting DNA sequence [3–10] and novel markers for the detection of hybridization event (markers those generated higher signals leading to higher sensitivity) [28], and formation of complex double stranded DNA structures (structures formed by multiple hybridization events) [29] causing to increment in the selectivity and sensitivity of the genosensors.

In this study, we report the fabrication of an electrochemical DNA sensor for detection of *L. infantum* genome. Non-spherical gold nanoparticles (ns-AuNPs) were prepared using an electrochemical deposition technique and employed as the electrochemical transducer of the DNA sensor. The developed DNA sensor in this study was successfully employed to examine clinical samples, exhibiting improved sensitivity, selectivity and analysis time compared with other available techniques.

2. Experimental section

All chemicals were purchased from Scharlau (Spain) or Sigma (USA) and were used without further purification. DNA oligonucleotide sequences were purchased from Cinaclon Co. (Iran). The oligonucleotides were dissolved in a 20 mmol L^{-1} Tris-HCl buffer solution (pH 7.4), aliquot into smaller volumes and stored at −20 °C.

A thiolated 26-base oligonucleotide sequence (p-ssDNA) was designed using NCBI BLAST nucleotide search tool and Primer3 based on a submitted sequence in GenBank (AB678348.1) of *L. infantum* minicircle kDNA (Iranian Standard strain MCAN/IR/97/LON490, isolate: IranJWinf) [30]. p-ssDNA was checked for any possible homology and shared sequences with any non-*L. infantum* species using the BLAST of NCBI. Moreover, the melting temperature of p-ssDNA was ensured to be within a narrow range using Oligo software. Then, the p-ssDNA sequence was checked for potential self-dimer and formation of secondary structures using mfold software (http://mfold.rna.albany.edu) [31] which may otherwise hinder the assay. Forward and reverse primers were employed for PCR.

Electrochemical experiments were carried out in a three-electrode cell containing a gold disk (Au) electrode (2 mm of diameter) covered with ns-AuNPs as the working electrode, a Pt wire counter electrode and an Ag/AgCl, 3 mol L^{-1} reference electrode, using a μ-Autolab potentiostat/galvanostat (the Netherlands) equipped with GPES software. Differential pulse voltammograms (DPVs) with a 25-mV pulse width, a 50-ms pulse time and a 10 mV s^{-1} of potential sweep rate were recorded for the DNA quantitation. PCR was carried out in a thermal cycler of Bio-Rad T100 (USA). The concentration of DNA samples were quantified using a NanoDrop™ Lite Spectrophotometer (USA).

Before electrodeposition of ns-AuNPs, the Au electrode surface

Please cite this article in press as: R. Nazari-Vanani, et al., Electrochemical quantitation of *Leishmania infantum* based on detection of its kDNA genome and transduction of non-spherical gold nanoparticles, Analytica Chimica Acta (2018), https://doi.org/10.1016/j.aca.2018.08.036

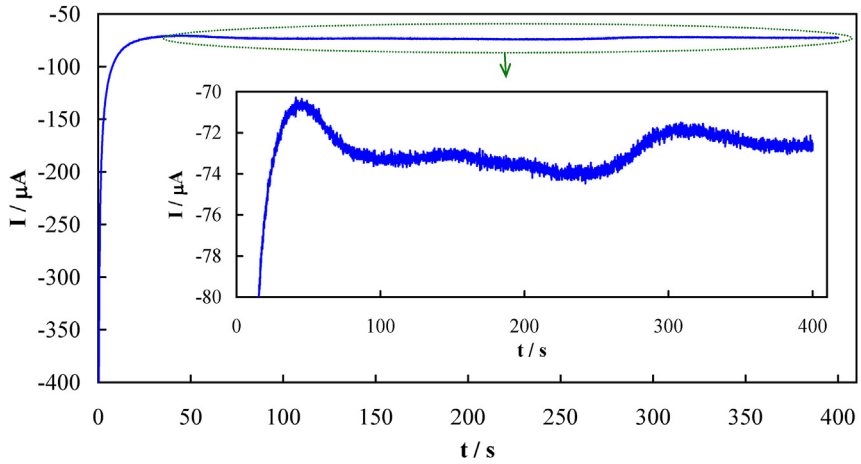

Fig. 1. A typical transient current-time curve during the electrodeposition of ns-AuNPs. The inset plot demonstrates the same curve with enlarged current axis.

was thoroughly polished with alumina powder and successively sonicated in an ethanol/water 3:1 (v/v) mixture for 5 min to eliminate surface contaminations. Afterward, the Au electrode surface was washed with distilled water. The electrode was then immersed into a solution comprising of 0.5 mol L^{-1} H_2SO_4, 20 mmol L^{-1} $HAuCl_4$ and 0.15 mol L^{-1} lactose. Electrodeposition was performed at 0.0 V vs. Ag/AgCl for 400 s. Then, the electrode was washed with distilled water and dried in air. The obtained electrode is denoted as Au/ns-AuNPs electrode throughout the text. Surface morphology of the electrodeposited ns-AuNPs was characterized by field emission scanning electron microscopy (FESEM) at different magnifications using a TESCAN Mira 3-XMU microscope (Czech Republic) with energy dispersive x-ray (EDX) analysis capability.

Before immobilization of p-ssDNA, a 10 μL of dithiothreitol (DTT) solution was added to a 10 μmol L^{-1} solution of p-ssDNA, mixed by a vortex and placed at ambient temperature for ~30 min. The excess DTT was removed with an equivalent volume of ethyl acetate. Then, 10 μL p-ssDNA solution was immediately dropped onto the surface of Au/ns-AuNPs electrode and incubated for at least 8 h at 4 °C. The electrode was then washed thoroughly with distilled water to remove the unconjugated DNA on the substrate. To attain a good orientation of p-ssDNA at the Au/ns-AuNPs electrode surface, the electrode was immersed into 1.0 mmol L^{-1} 6-mercapto-1-hexanol for 30 min and then rinsed thoroughly with redistilled water. The obtained electrode is denoted as the DNA sensor. Open-circuit potential (OCP) measurements were performed using gold screen-printed electrodes (DropSens, Spain) covered by ns-AuNPs to optimize the immobilization time of p-ssDNA. A 10 μmol L^{-1} solution of p-ssDNA was precisely dropped on the electrode surface and kept refrigerated at 4 °C for >5 h while continuously recording OCP by a digital multimeter.

To quantify the p-ssDNA complementary oligonucleotide (target sequence, t-ssDNA) using the DNA sensor, a stock solution of t-ssDNA was prepared, and a serial dilution was then made in the range of 1.0×10^{-10} to 1.0×10^{-18} mol mL^{-1}. Hybridization process between the immobilized p-ssDNA and t-ssDNA was carried out by dropping different t-ssDNA concentrations onto the DNA sensor surface for 40 min at 37 °C [5]. Then, the DNA sensor was rinsed with distilled water to remove the unhybridized t-ssDNA, placed in a toluidine blue (TB) solution comprising 20 μmol L^{-1} TB dissolved in Tris (as a redox indicator) for 5 min, rinsed again with distilled water, placed in Tris, and subjected to DPV measurements. DPVs were also recorded before the hybridization of DNA sensor with t-ssDNA. The peak currents in DPVs (related to the reduction of TB bound to single stranded or double stranded DNA) were employed to quantify the DNA concentrations. A calibration curve was plotted for quantitation of t-ssDNA by the DNA sensor.

The fabrication reproducibility of the DNA sensor was investigated by dipping the DNA sensor in the Piranha solution for 30 s, followed by re-fabrication of the DNA sensor. This procedure was repeated multiple times and DPVs for the repeating fabrication were recorded. The DNA sensor regeneration was determined by performing five hybridization/dehybridization cycles of 1.0×10^{-12} mol L^{-1} t-ssDNA. After each hybridization step, the DNA sensor was placed in water at 95 °C for 5 min to de-hybridize the formed double stranded DNA. Next, it was re-hybridized with the same t-ssDNA concentration. At each cycle, DPVs were recorded before and after hybridization. To evaluate the stability of the DNA sensor, DPVs for 1.0×10^{-13} mol L^{-1} t-ssDNA was monitored at regular intervals. After taking each DPV, the DNA sensor was placed in Tris at 4 °C.

The cryopreserved *Leishmania major* (MRHO/IR/75/ER) and *L. infantum* (MCAN/IR/96/LON49) and *Leishmania tropica* (MHOM/IR/02/Mash10) were received from Tehran University of Medical Sciences, Tehran, Iran, and cultivated in RPMI 1640 medium supplemented with 10% (v/v) heat-inactivated fetal bovine serum (Gibco) and 1% pen-strep (Sigma) at 24 °C. A concentration of 1×10^7 mL^{-1} of parasites was reached following the daily counting of promastigotes in a Neubauer chamber. The culture was centrifuged to collect around 10^7 phase promastigotes of isolates. The resultant pellets were washed 3–4 times using refrigerated 50 mmol L^{-1} phosphate buffer saline (pH 7.0 and 0.7% NaCl) and then dispersed in 750 mL of NET buffer (5 mol L^{-1} NaCl, 0.5 mol L^{-1} EDTA, 1 mol L^{-1} Tris buffer pH 8.0). The cells were lysed using Proteinase K (100 mg mL^{-1}) and 1% sodium dodecyl sulphate for 3–4 h at 56 °C. The samples were transferred into a YTA Genomic DNA extraction mini kit (Yekta Tajhiz Azma, Iran) and total DNA was extracted following the manufacturer's instructions. The obtained DNA was diluted in 100–150 μL of elution buffer. The concentration of parasitic DNA was determined by a Thermo Scientific NanoDrop 2000c (USA) and then diluted to a desired value.

To evaluate the selectivity of the DNA sensor, sequences of single-, double- and three-base mismatched sequences (1-t-ssDNA, 2-t-ssDNA and 3-t-ssDNA) with a concentration of 1.0×10^{-12} mol L^{-1} were hybridized with the DNA sensor. The response of the DNA sensor for mismatched sequences were compared together and with that of t-ssDNA. In addition, *Leishmania tropica* (*L. tropica*) and *Leishmania major* (*L. major*) genomic DNA was prepared and analyzed with the DNA sensor using a similar procedure employed for determination of *L. infantum* genomic DNA (vide infra).

Please cite this article in press as: R. Nazari-Vanani, et al., Electrochemical quantitation of *Leishmania infantum* based on detection of its kDNA genome and transduction of non-spherical gold nanoparticles, Analytica Chimica Acta (2018), https://doi.org/10.1016/j.aca.2018.08.036

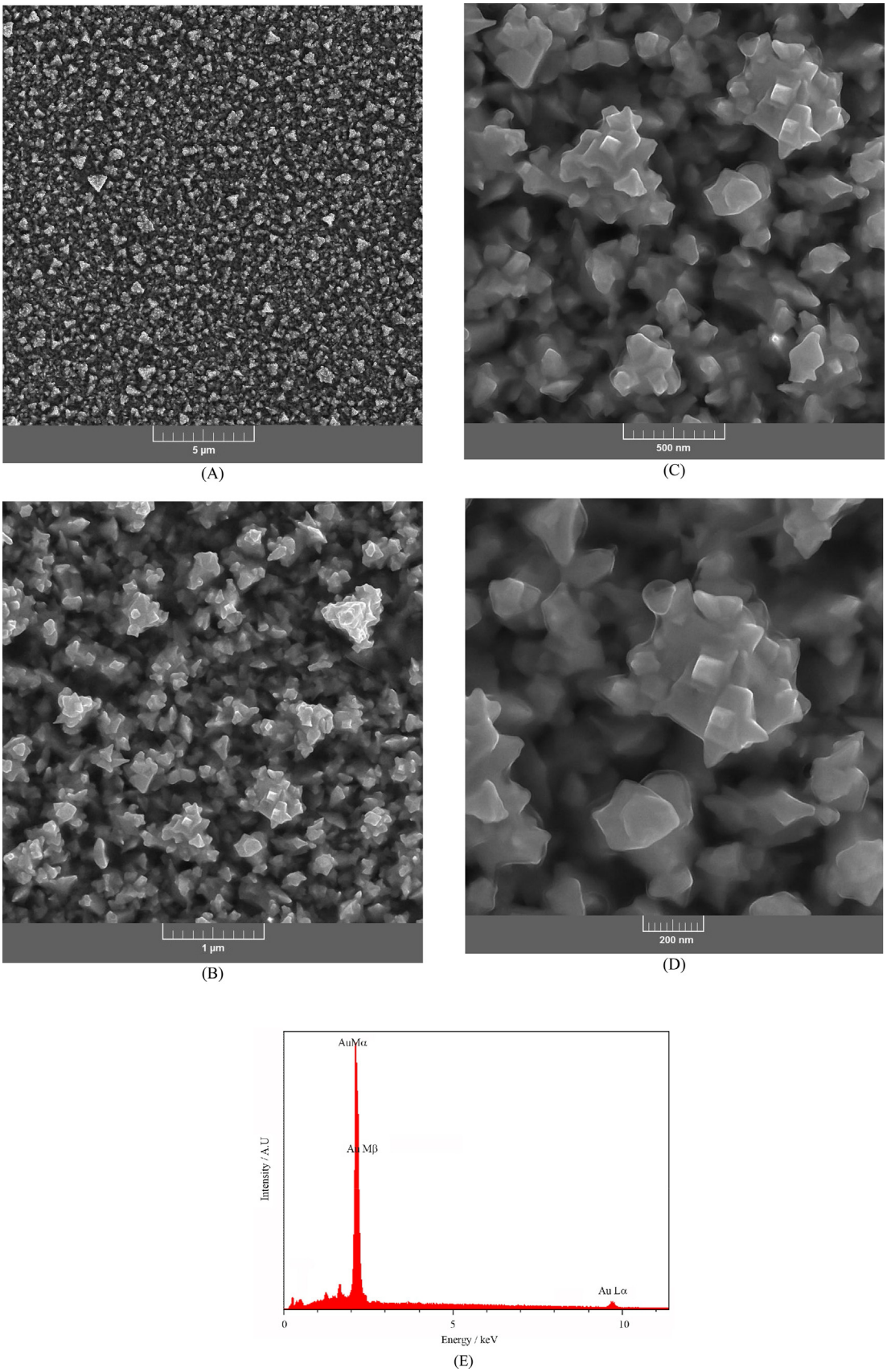

Fig. 2. (A-D) SEM micrographs of as-prepared ns-AuNPs electrode at different magnifications; (E) EDX analysis of the electrode surface.

Please cite this article in press as: R. Nazari-Vanani, et al., Electrochemical quantitation of *Leishmania infantum* based on detection of its kDNA genome and transduction of non-spherical gold nanoparticles, Analytica Chimica Acta (2018), https://doi.org/10.1016/j.aca.2018.08.036

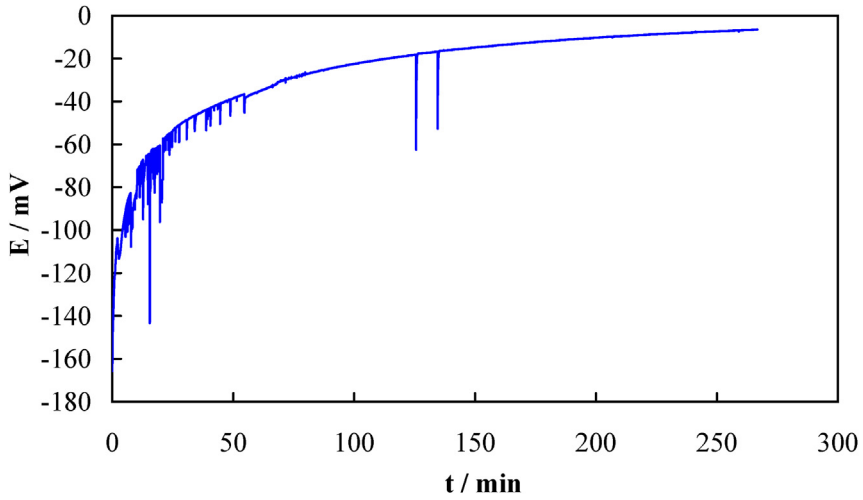

Fig. 3. The OCP of the ns-AuNPs electrode recorded versus time during the immobilization process of p-ssDNA at the electrode surface over a 6 h period.

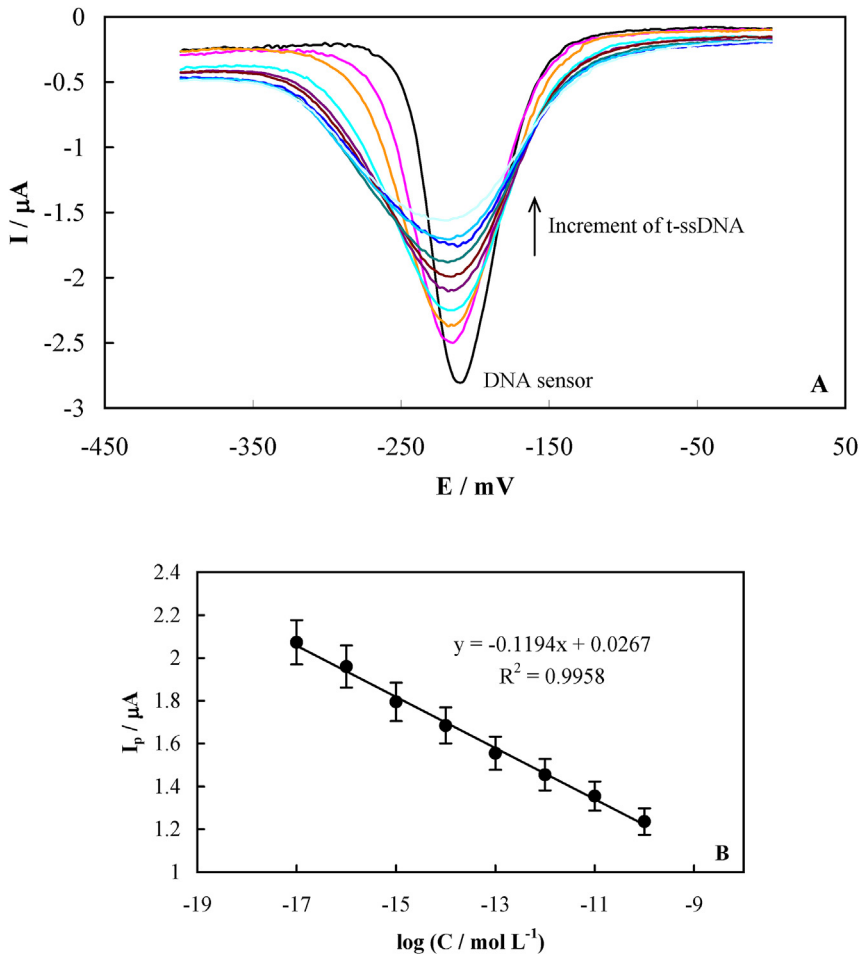

Fig. 4. (A) DPVs of bound TB before (DPV with the highest peak current) and after hybridization of the DNA sensor with different concentrations of t-ssDNA sequence; (B) the linear correlation between the peak current for DPVs shown in panel (A) with t-ssDNA concentration within the dynamic range of 1×10^{-18} to 1×10^{-10} mol L^{-1}.

Please cite this article in press as: R. Nazari-Vanani, et al., Electrochemical quantitation of *Leishmania infantum* based on detection of its kDNA genome and transduction of non-spherical gold nanoparticles, Analytica Chimica Acta (2018), https://doi.org/10.1016/j.aca.2018.08.036

Table 1
A comparison between various detection methods of *L. infantum*.

Detection method	Nanomaterial employed	Linear range	LOD	Sensitivity	Reference
Electrochemical impedance	Carbon Nanotubes	0.1–98.3 fg μL $^{-1}$	15 fmol L^{-1}	–	[32]
Electrochemical impedance	Gold nanoparticles	0.01 pg mL^{-1} - 10 ng mL^{-1}		–	[33]
Surface plasmon resonance immunosensing	Gold nanoparticles	1–300 nmol L^{-1}	0.41 nmol L^{-1}	–	[34]
PCR enzyme-linked immunosorbent assay	–	–	50-100 promastigotes	1 fg	[35]
PCR enzyme-linked immunosorbent assay	–	0.07–700 fg	0.07 fg	100%	[36]
Electrochemical DNA sensor[a]	Non-spherical gold nanoparticles	10 amol L^{-1} - 0.1 nmol L^{-1}	0.2 amol L^{-1}	−0.1194 μA/[log (C^{b}/mol L^{-1})]	This study
Electrochemical DNA sensor[c]	Non-spherical gold nanoparticles	15–50 ng μL^{-1}	9 ng μL^{-1}	−2.4432 μA/[log (C^{d}/ng μL^{-1})]	This study

[a] For the detection of t-ssDNA.
[b] Concentration of t-ssDNA in mol L-1.
[c] For the detection of genomic DNA.
[d] Concentration of genomic DNA in ng μL^{-1}.

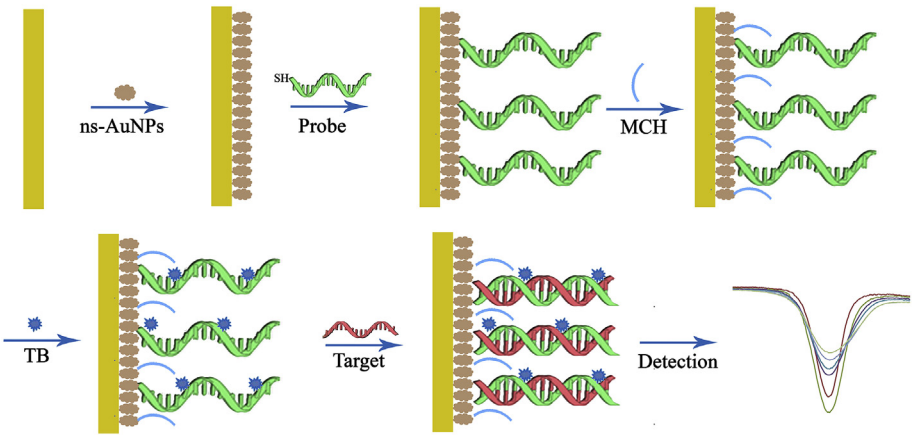

Scheme 1. The fabrication and operation steps of the DNA sensor.

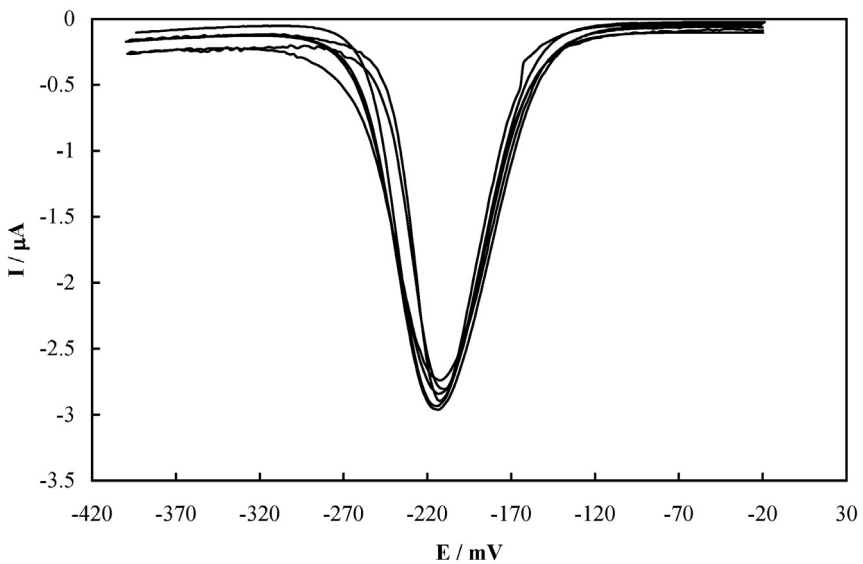

Fig. 5. DPVs of the reproduced DNA sensor via dipping the electrode in the Piranha solution for 30 s, followed by re-fabrication process.

Please cite this article in press as: R. Nazari-Vanani, et al., Electrochemical quantitation of *Leishmania infantum* based on detection of its kDNA genome and transduction of non-spherical gold nanoparticles, Analytica Chimica Acta (2018), https://doi.org/10.1016/j.aca.2018.08.036

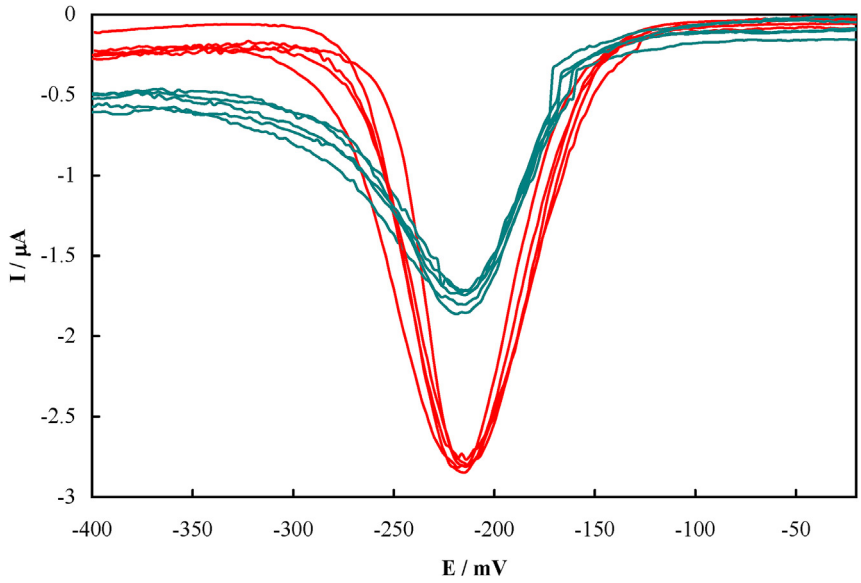

Fig. 6. DPVs obtained before and after repeated cycles of hybridization/dehybridization using t-ssDNA (1.0×10^{-12} mol L^{-1}).

The oligonucleotide sequences used in the present study are as follows:

p-ssDNA sequence: 5′ SH-$(CH_2)_6$-ATCTCGTAAGCA-GATCGCTGTGTCAC 3'

t-ssDNA sequence: 5′ GTGACACAGCGATCTGCTTACGAGAT 3'

1-t-ssDNA sequence: 5′ CTGACACAGCGATCTGCTTACGAGAT 3'

2-t-ssDNA sequence: 5′ CCGACACAGCGATCTGCTTACGAGAT 3'

3-t-ssDNA sequence: 5′ CCCACACAGCGATCTGCTTACGAGAT 3'

Forward PCR primer: 5′ CCACCCGGCCCTATTTTACA 3'

Reverse PCR primer: 5′ GGCTGAAGCCTGTTAGTGGT 3'

In order to determine the *L. infantum* standard genomic DNA, different concentrations of DNA in the range of 0.5–30 ng μL^{-1} were placed in water at 95 °C for 5 min to de-hybridize. Then, the DNA solutions were hybridized with the DNA sensor and DPVs were recorded after binding with TB (vide supra, as depicted for t-ssDNA quantitation). A calibration curve was plotted to evaluate the detection characteristics of genomic DNA by the DNA sensor.

DNA analysis in clinical samples was performed to confirm the applicability of the DNA sensor for practical samples. Clinical specimens including one human sample and 8 buffy coat samples from pet dogs with cutaneous lesions were analyzed. All these samples were previously confirmed to be infected with *L. infantum* by PCR followed by gel electrophoreses. The genomic DNA from these samples was extracted using commercially available kit from CinnaGen (Iran). DNA extraction and purification were performed according to the kit manufacturer. All samples were kept in microtubes and used directly without any pretreatment.

3. Results and discussion

The DNA sensor transducer composed of ns-AuNPs and was synthesized using an electrochemical deposition method under potentiostatic conditions. A typical transient current-time curve during the electrodeposition process is shown in Fig. 1. The curve represents a non-zero initial current related to instantaneous nucleation, followed by a sharp decrement due to the early formation of the nuclei on the Au electrode surface. Then, the current slightly increases due to the formation and growth of ns-AuNPs. Subsequently, the current reaches to a steady plateaued indicating continual growth of ns-AuNPs.

To investigate morphology of ns-AuNPs synthesized in the presence of lactose, the electrode surface was inspected by FESEM. The recorded images at different magnifications (Fig. 2A–D) illustrate that the electrode surface is covered by a uniform layer of non-spherical gold nanoparticles with a mean dimension of 80 ± 20 nm. In addition, EDX analysis (Fig. 2E) confirms the formation of a gold layer with high chemical purity. This configuration of the gold nanostructure provides high surface area for immobilization of p-ssDNA at the electrode surface. The real surface area of the Au/ns-AuNPs electrode was electrochemically measured using cyclic voltammetry in a $K_4Fe(CN)_6/K_3Fe(CN)_6$ solution (Supplementary Fig. S1). The real surface area for the Au/ns-AuNPs electrode was obtained to be 0.27 cm^2, exhibiting a roughness factor of 8.6.

The DNA sensor was prepared by immobilization of p-ssDNA on the Au/ns-AuNPs electrode. The immobilization time was optimized by monitoring the OCP for the electrode over a 6 h period (Fig. 3). In a typical experiment, the immobilization process was completed within ~300 min, determined by the steady potential of the electrode. Thus, an optimized immobilization time of 5 h was applied to prepare the DNA sensor throughout the study. The DNA sensor was then incubated with t-ssDNA solution with different concentrations for 40 min at 37 °C to conduct the hybridization detection and recording readout signals. The DNA sensor displayed a decrease in TB reduction signal upon hybridization of the t-ssDNA, indicating that t-ssDNA is bound onto the DNA sensor surface. Fig. 4A shows DPVs of bound TB before and after hybridization of the DNA sensor with different concentrations of t-ssDNA sequence. The DPV response of the DNA sensor exhibits a linear correlation with the logarithm of t-ssDNA concentration (Fig. 4B) within a dynamic range of 1×10^{-18} to 1×10^{-10} mol L^{-1}. The limit of detection (LOD) was calculated based on S-(3 × SD), where S and SD are the average and the standard deviation of the DNA sensor signal in the absence of t-ssDNA, respectively. The LOD of the DNA sensor for the detection of t-ssDNA was obtained as 2×10^{-19} mol L^{-1}. Different techniques employed for detection of *L. infantum* are compared in Table 1. The comparison presented in Table 1 reveals that the developed DNA sensor in this study demonstrates improved detection criteria for *L. infantum* parasite. The fabrication and operation steps of the DNA sensor were presented in Scheme 1.

Please cite this article in press as: R. Nazari-Vanani, et al., Electrochemical quantitation of *Leishmania infantum* based on detection of its kDNA genome and transduction of non-spherical gold nanoparticles, Analytica Chimica Acta (2018), https://doi.org/10.1016/j.aca.2018.08.036

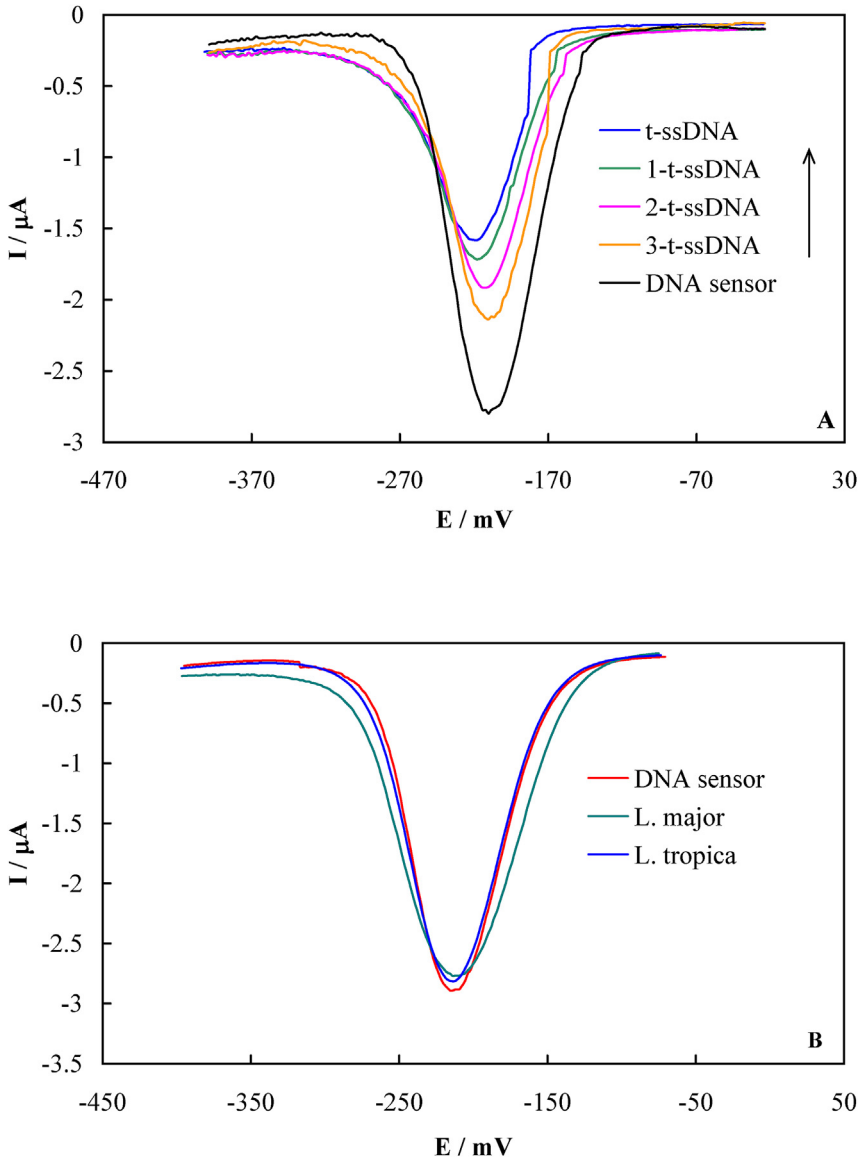

Fig. 7. DPVs of bound TB measured using the DNA sensor before (DPV with the highest peak current) and after hybridization with (A) t-ssDNA, 1-t-ssDNA, 2-t-ssDNA and 3-t-ssDNA and (B) genomic DNA from *L. tropica* and *L. Major*.

The fabrication reproducibility of the DNA sensor was explored according to the procedure explained in the experimental section. The resulted DPV responses for reproduction of the DNA sensor are presented in Fig. 5. A relative standard deviation of ~4.5% was obtained for the DNA sensor signals during repeating fabrication process. These results indicate the excellent reproducibility of the developed DNA sensor. The regeneration ability of the DNA sensor was also investigated by conducting consecutive hybridization/dehybridization cycles. Fig. 6 shows DPVs obtained before and after repeated hybridization/dehybridization using t-ssDNA. The DNA biosensor exhibited DPV peaks with ~5.2% of its original current, suggesting acceptable regeneration ability.

The selectivity of a sensor to distinguish t-ssDNA among other similar species is another significant determining parameter for its practicality. The selectivity of the DNA sensor was verified by hybridization with different DNA sequences. Fig. 7A depicts DPVs recorded using the DNA sensor before and after hybridization with t-ssDNA, 1-t-ssDNA, 2-t-ssDNA and 3-t-ssDNA. The DNA sensor exhibits the lowest peak current for t-ssDNA, whereas the DPV peak

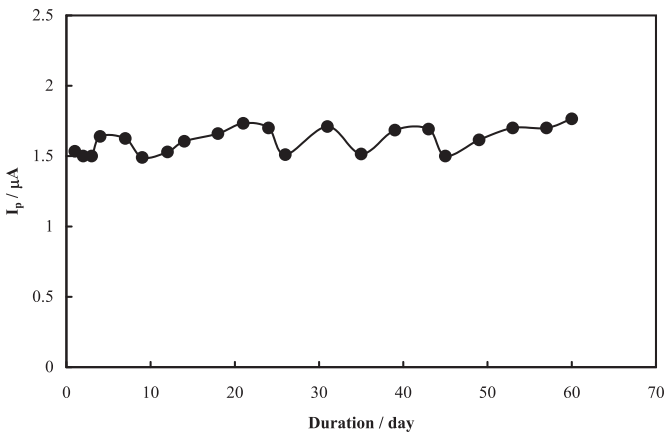

Fig. 8. The analytical response of the DNA sensor recorded during consecutive days.

Please cite this article in press as: R. Nazari-Vanani, et al., Electrochemical quantitation of *Leishmania infantum* based on detection of its kDNA genome and transduction of non-spherical gold nanoparticles, Analytica Chimica Acta (2018), https://doi.org/10.1016/j.aca.2018.08.036

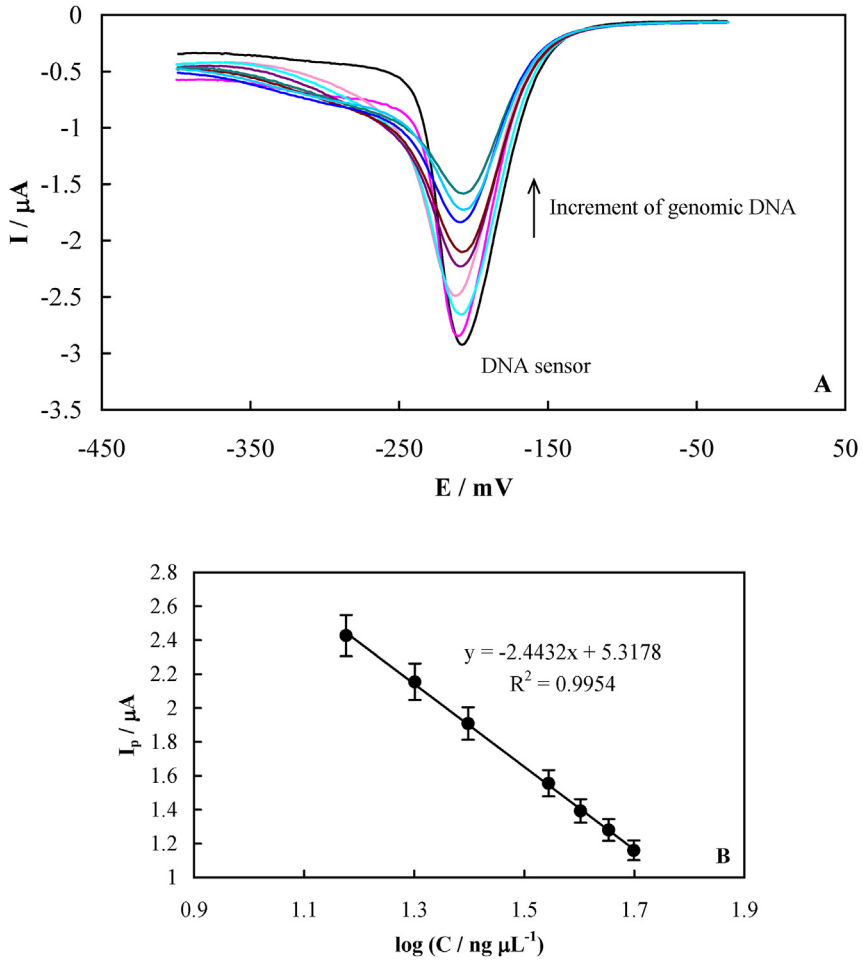

Fig. 9. (A) DPVs of bound TB before (DPV with the highest peak current) and after hybridization of the DNA sensor with different concentrations of genomic DNA from *L. infantum*; (B) the linear correlation between the peak current for DPVs shown in panel (A) with genome concentration within the dynamic range of 15–50 ng μL^{-1}.

current increases with increase of the mismatch level in the DNA sequences. Assuming the t-ssDNA hybridization efficiency of 100%, the hybridization efficiencies for 1-t-ssDNA, 2-t-ssDNA and 3-t-ssDNA are estimated as 88, 74 and 54%, respectively. In addition, genomic DNA from *L. tropica* and *L. major* were analyzed with the DNA sensor for which the related DPVs are shown in Fig. 7B. The results indicate that the DNA sensor did not respond to *L. tropica* and *L. Major*, illustrating the good selectivity of the developed sensor toward t-ssDNA.

The analytical response of the DNA sensor was recorded during consecutive days to examine the stability of the sensor (Fig. 8). The DNA sensor maintained a relatively constant response within 60 days with minor random fluctuations. Accordingly, the storage period of the DNA sensor is considered to be 2 months.

The electrochemical response of the DNA sensor for analytical measurement of extracted genomic DNA from *L. infantum* was also investigated. A stock solution of the genome was prepared according to the procedure described in the experimental section, followed by a serial dilution to prepare different concentrations ranging from 10 to 50 ng μL^{-1}. Fig. 9A shows the DPVs of bound TB before and after hybridization of the DNA sensor with the genome. The DPV response of the DNA sensor exhibits a linear correlation with the logarithm of genome concentration in a dynamic range of 15–50 ng μL^{-1} (Fig. 9B). The LOD of the DNA sensor for the detection of genomic DNA was obtained to be 9 ng μL^{-1} (see also Table 1).

In order to apply the DNA sensor for detection of the pathogen in real samples, clinical specimens were collected, the corresponding genome was extracted and the resulting samples were directly analyzed by the DNA sensor without any pretreatment (e.g. PCR amplification). The limit of quantitation (LOQ) for a given analytical technique is defined as a concentration for which a signal equal to 10 × SD is produced [37]. Accordingly, we considered a sample to be positive when the DNA sensor produces a signal ≤ S-10 × SD. The developed DNA sensor in this study successfully recognized the positive samples, indicating the applicability of the DNA sensor for clinical analysis of real samples.

4. Conclusion

A DNA sensor was designed and developed based on the hybridization of a single-stranded DNA of *L. Infantum* immobilized on the gold nanostructures and toluidine blue as a redox indicator. The developed DNA sensor demonstrated a linear correlation for electrochemical response in a DPV regime with the concentration of t-ssDNA in a wide range from 1×10^{-18} to 1×10^{-10} mol L^{-1} with the LOD of 2×10^{-19} mol L^{-1}. The obtained LOD using the developed DNA sensor in this study is the lowest among the available clinical techniques. In addition, the presented DNA sensor was successfully applied for diagnosis of *L. Infantum* in clinical samples. Compared with the other available techniques, the developed DNA sensor in this study provides higher sensitivity, improved selectivity, shorter analysis time and ease of fabrication and application.

Please cite this article in press as: R. Nazari-Vanani, et al., Electrochemical quantitation of *Leishmania infantum* based on detection of its kDNA genome and transduction of non-spherical gold nanoparticles, Analytica Chimica Acta (2018), https://doi.org/10.1016/j.aca.2018.08.036

Acknowledgments

Research reported in this publication was supported by Elite Researcher Grant Committee under award number [958749] from the National Institutes for Medical Research Development (NIMAD), Tehran, Iran. We would also like to thank the Research Consultation Center of Shiraz University of Medical Sciences.

Appendix A. Supplementary data

Supplementary data related to this article can be found at https://doi.org/10.1016/j.aca.2018.08.036.

References

[1] L. Varadi, J.L. Luo, D.E. Hibbs, J.D. Perry, R.J. Anderson, S. Orenga, P.W. Groundwater, Methods for the detection and identification of pathogenic bacteria: past, present, and future, Chem. Soc. Rev. 46 (2017) 4818–4832.
[2] D.V. Lim, Detection of microorganisms and toxins with evanescent wave fiber-optic biosensors, Proc. IEEE 91 (2003) 902–907.
[3] A. Rahi, N. Sattarahmady, H. Heli, Zepto-molar electrochemical detection of Brucella genome based on gold nanoribbons covered by gold nanoblooms, Sci. Rep. 5 (2015) 18060.
[4] N. Sattarahmady, A. Movahedpour, H. Heli, G.R. Hatam, Gold nanoparticles-based biosensing of Leishmania major kDNA genome: visual and spectrophotometric detections, Sensor. Actuator. B 235 (2016) 723–731.
[5] H. Heli, N. Sattarahmady, G.R. Hatam, F. Reisi, R.D. Vais, An electrochemical genosensor for Leishmania major detection based on dual effect of immobilization and electrocatalysis of cobalt-zinc ferrite quantum dots, Talanta 156 (2016) 172–179.
[6] M. Moradi, N. Sattarahmady, A. Rahi, G.R. Hatam, S.M.R. Sorkhabadi, H. Heli, A label-free, PCR-free and signal-on electrochemical DNA biosensor for Leishmania major based on gold nanoleaves, Talanta 161 (2016) 48–53.
[7] A. Rahi, N. Sattarahmady, H. Heli, An ultrasensitive electrochemical genosensor for Brucella based on palladium nanoparticles, Anal. Biochem. 510 (2016) 11–17.
[8] N. Sattarahmady, G.H. Tondro, M. Golchin, H. Heli, Gold nanoparticles biosensor of Brucella spp. genomic DNA: visual and spectrophotometric detections, Biochem. Eng. J. 97 (2015) 1–7.
[9] M. Moradi, N. Sattarahmady, G.R. Hatam, H. Heli, Electrochemical genosensing of Leishmania major using gold hierarchical nanoleaflets, J. Biol. Today's World 5 (2016) 128–136.
[10] J. Mohammadi, A. Moattari, N. Sattarahmady, N. Pirbonyeh, H. Yadegari, H. Heli, Electrochemical biosensing of influenza A subtype genome based on meso/macroporous cobalt (II) oxide nanoflakes-applied to human samples, Anal. Chim. Acta 979 (2017) 51–57.
[11] S. Sundar, M. Rai, Laboratory diagnosis of visceral leishmaniasis, Clin. Diagn. Lab. Immunol. 9 (2002) 951–958.
[12] E. Ismail, V. Bogdanova, G. Shopov, S. Dobrev, N. Ivanova, Kala-azar: nature, biophysical aspects, clinical manifestation and treatment, J. Pharm. Pharmacol. 6 (2017) 33–36.
[13] P.J. Guerin, P. Olliaro, S. Sundar, M. Boelaert, S.L. Croft, P. Desjeux, M.K. Wasunna, A.D.M. Bryceson, Visceral leishmaniasis: current status of control, diagnosis, and treatment, and a proposed research and development agenda, Lancet Infect. Dis. 2 (2002) 494–501.
[14] F. Dantas-Torres, K.G.D. Sales, L.G. da Silva, D. Otranto, L.A. Figueredo, Leishmania-FAST15: a rapid, sensitive and low-cost real-time PCR assay for the detection of Leishmania infantum and Leishmania braziliensis kinetoplast DNA in canine blood samples, Mol. Cell. Probes 31 (2017) 65–69.
[15] A.C. Rosypal, G.C. Troy, A.M. Zajac, R.B. Duncan, K. Waki, K.P. Chang, D.S. Lindsay, Emergence of zoonotic canine leishmaniasis in the United States: isolation and immunohistochemical detection of Leishmania infantum from foxhounds from Virginia, J. Eukaryot. Microbiol. 50 (2003) 691–693.
[16] S. Reale, L. Maxia, F. Vitale, N.S. Glorioso, S. Caracappa, G. Vesco, Detection of Leishmania infantum in dogs by PCR with lymph node aspirates and blood, J. Clin. Microbiol. 37 (1999) 2931–2935.
[17] F. Chappuis, S. Sundar, A. Hailu, H. Ghalib, S. Rijal, R.W. Peeling, J. Alvar, M. Boelaert, Visceral leishmaniasis: what are the needs for diagnosis, treatment and control? Nat. Rev. Microbiol. 5 (2007) 873–882.
[18] G. Cabral-Miranda, J.R. de Jesus, P.R.S. Oliveira, G.S.G. Britto, L.C. Pontes-de-Carvalho, R.F. Dutra, N.M. Alcantara-Neves, Detection of parasite sntigens in Leishmania infantum-infected spleen tissue by monoclonal antibody-, piezoelectric-based immunosensors, J. Parasitol. 100 (2014) 73–78.
[19] S. Liebana, D. Brandao, P. Cortes, S. Campoy, S. Alegret, M.I. Pividori, Electrochemical genosensing of Salmonella, Listeria and Escherichia coli on silica magnetic particles, Anal. Chim. Acta 904 (2016) 1–9.
[20] L. Solano-Gallego, A. Rodriguez-Cortes, M. Trotta, C. Zampieron, L. Razia, T. Furlanello, M. Caldin, X. Roura, J. Alberola, Detection of Leishmania infantum DNA by fret-based real-time PCR in urine from dogs with natural clinical leishmaniosis, Vet. Parasitol. 147 (2007) 315–319.
[21] A.L.C. Ferreira, V.M. Carregal, S.D. Ferreira, R.S. Leite, A.S.R. de Andrade, Detection of Leishmania infantum in 4 different dog samples by real-time PCR and ITS-1 nested PCR, Diagn, Microorg. Infect. Dis. 78 (2014) 418–421.
[22] D.E.P. Souto, J.V. Silva, H.R. Martins, A.B. Reis, R.C.S. Luz, L.T. Kubota, F.S. Damos, Development of a label-free immunosensor based on surface plasmon resonance technique for the detection of anti-Leishmania infantum antibodies in canine serum, Biosens. Bioelectron. 46 (2013) 22–29.
[23] M.F. Persichetti, L. Solano-Gallego, A. Vullo, M. Masucci, P. Marty, P. Delaunay, F. Vitale, M.G. Pennisi, Diagnostic performance of ELISA, IFAT and Western blot for the detection of anti-Leishmania infantum antibodies in cats using a Bayesian analysis without a gold standard, Parasites Vectors 10 (2017) 119.
[24] A. Rahi, K. Karimian, H. Heli, Nanostructured materials in electroanalysis of pharmaceuticals, Anal. Biochem. 497 (2016) 39–47.
[25] H. Heli, A. Rahi, Synthesis and applications of nanoflowers, recent pat, Nanotechnology 10 (2016) 86–115.
[26] H. Heli, M. Negahdary, Applications of nanoflowers in biomedicine, recent pat, Nanotechnology (2017), https://doi.org/10.2174/1872210511666170911153428.
[27] G.S. Shruthi, C.V. Amitha, B.B. Mathew, Biosensors: a modern day achievement, J. Instrum. Technol. 2 (2014) 26–39.
[28] R. Ziolkowski, A.B. Olejniczak, L. Gorski, J. Janusik, Z.J. Lesnikowski, E. Malinowska, Electrochemical detection of DNA hybridization using metallacarborane unit, Bioelectrochemistry 87 (2012) 78–83.
[29] S. Li, W. Qiu, X. Zhang, J. Ni, F. Gao, Q. Wang, A high-performance DNA biosensor based on the assembly of gold nanoparticles on the terminal of hairpin-structured probe DNA, Sensor. Actuator. B 223 (2016) 861–867.
[30] S. Khademvatan, N. Neisi, S. Maraghi, J. Saki, Diagnosis and identification of Leishmania spp. From Giemsa-stained slides, by real-time PCR and melting-curve analysis in south-west of Iran, Ann. Trop. Med. Parasitol. 105 (2011) 559–565.
[31] M. Zuker, Mfold web server for nucleic acid folding and hybridizationprediction, Nucleic Acids Res. 33 (2003) 3406–3415.
[32] I.A.M. Frias, C.A.S. Andrade, V.Q. Balbino, C.P. de Melo, Use of magnetically disentangled thiolated carbon nanotubes as a label-free impedimetric genosensor for detecting canine Leishmania spp. infection, Carbon 117 (2017) 33–40.
[33] M.F.K.D. Garcia, C.A.S. Andrade, C.P. De Melo, D.S. Gomes, L.G. Silva, R.V. Dias, V.Q. Balbino, M.D.L. Oliveira, Impedimetric sensor for Leishmania infantum genome based on gold nanoparticles dispersed in polyaniline matrix, J. Chem. Technol. Biotechnol. 91 (2016) 2810–2816.
[34] S.Y. Neto, D.E. P Souto, H.M. de Andrade, R.D.C. S Luz, L.T. Kubota, F.S. Damos, Visible LED light driven photoelectroanalytical detection of antibodies of visceral leishmaniasis based on electrodeposited CdS film sensitized with Au nanoparticles, Sens. Actuators, B 256 (2018) 682–690.
[35] J. Martin-Sanchez, M.C. Lopez-Lopez, C. Acedo-Sanchez, J.J. Castro-Fajardo, J.A. Pineda, F. Morillas-Marquez, Diagnosis of infections with Leishmania infantum using PCR-ELISA, Parasitology 122 (2001) 607–615.
[36] F.A.C. Medeiros, L.I. Gomes, E. Oliveira, C.S.A. de Souza, M.V. Mourao, G.F. Cota, L.H.D. Marques, M. Carneiro, A. Rabello, Development and validation of a PCR-ELISA for the diagnosis of symptomatic and asymptomatic infection by Leishmania (Leishmania) infantum, J. Trop. Med. 2017 (2017) 1–10.
[37] J. Miller, Statistics for Analytical Chemistry, Prentice Hall, 1993.